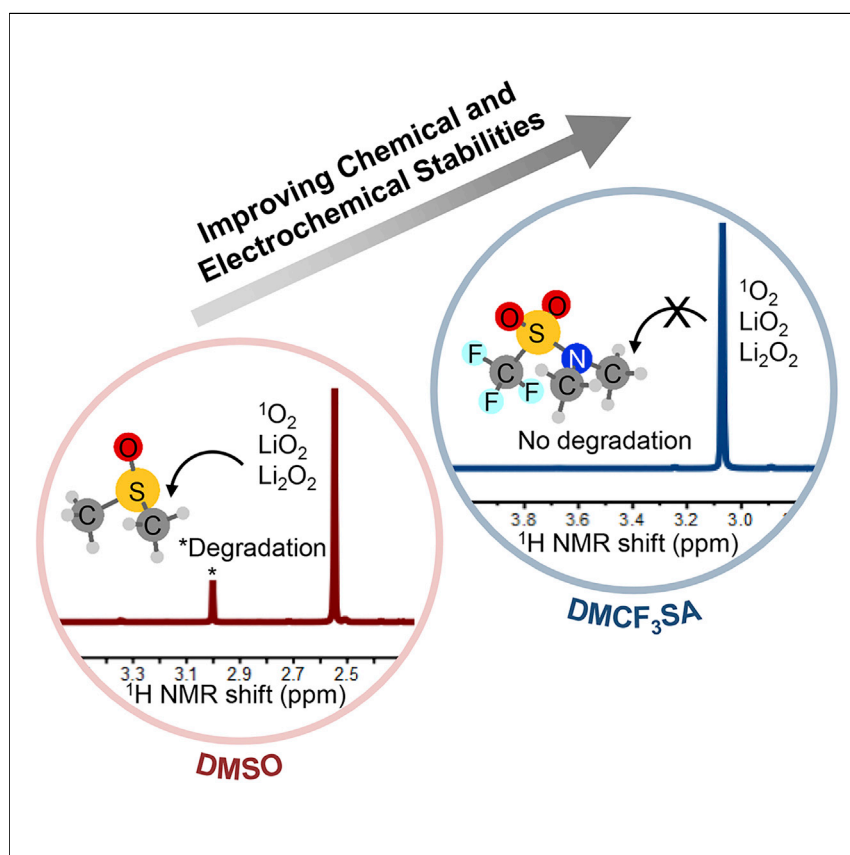


## Article

Molecular Design of Stable Sulfamide- and Sulfonamide-Based Electrolytes for Aprotic Li-O<sub>2</sub> Batteries

Aprotic lithium-oxygen (Li-O<sub>2</sub>) batteries show great promise in energy storage and transportation applications because of their high gravimetric energies, which potentially represent a several-fold increase over Li-ion batteries. The stable and reversible operation of Li-O<sub>2</sub> batteries, however, is currently hindered by the severe degradation of common electrolytes. Here, we show that sulfonamide-based electrolytes, designed on the basis of physical organic chemistry principles, can exhibit higher (electro)chemical stability than common electrolytes, such as tetraglyme and DMSO.

Shuting Feng, Mingjun Huang, Jessica R. Lamb, ..., Collin F. Perkinson, Jeremiah A. Johnson, Yang Shao-Horn

fengs@mit.edu (S.F.)  
jaj2109@mit.edu (J.A.J.)

## HIGHLIGHTS

Designed electrolytes are highly resistant to chemical degradation by (su)peroxide

Sulfonamide-based electrolytes showed electrochemical oxidative stability at >4.2V<sub>Li</sub>

Sulfonamides showed higher cycling stability than tetraglyme and DMSO

Article

# Molecular Design of Stable Sulfamide- and Sulfonamide-Based Electrolytes for Aprotic Li-O<sub>2</sub> Batteries

Shuting Feng,<sup>1,5,\*</sup> Mingjun Huang,<sup>2,5</sup> Jessica R. Lamb,<sup>2</sup> Wenxu Zhang,<sup>2</sup> Ryoichi Tatara,<sup>3</sup> Yirui Zhang,<sup>4</sup> Yun Guang Zhu,<sup>3</sup> Collin F. Perkinson,<sup>2</sup> Jeremiah A. Johnson,<sup>2,6,\*</sup> and Yang Shao-Horn<sup>3,4</sup>

## SUMMARY

Electrolyte instability is one of the most challenging impediments to enabling lithium-oxygen (Li-O<sub>2</sub>) batteries for practical use. The use of physical organic chemistry principles to rationally design new molecular components may enable the discovery of electrolytes with stability profiles that cannot be achieved with existing formulations. Here, we report on the development of sulfamide- and sulfonamide-based small molecules that are liquids at room temperature, capable of dissolving reasonably high concentration of Li salts (e.g., lithium bis(trifluoromethane)sulfonimide [LiTFSI]), and exceptionally stable under the harsh chemical and electrochemical conditions of aprotic Li-O<sub>2</sub> batteries. In particular, *N,N*-dimethyl-trifluoromethanesulfonamide was found to be highly resistant to chemical degradation by peroxide and superoxide, stable against electrochemical oxidation up to 4.5 V<sub>Li</sub>, and stable for >90 cycles in a Li-O<sub>2</sub> cell when cycled at <4.2 V<sub>Li</sub>. This study provides guiding principles for the development of next-generation electrolyte components based on sulfamides and sulfonamides.

## INTRODUCTION

Aprotic lithium-oxygen (Li-O<sub>2</sub>) batteries show great promise in energy storage and transportation applications because of their high gravimetric energies, which potentially represent a 3- to 5-fold increase over Li-ion batteries.<sup>1–4</sup> The stable and reversible operation of Li-O<sub>2</sub> batteries is currently hindered by the severe degradation of common electrolytes. Indeed, many of the commonly used electrolyte components of well-established battery chemistries (e.g., Li ion), such as carbonates,<sup>5–8</sup> glymes,<sup>9–11</sup> dimethyl sulfoxide (DMSO),<sup>12–14</sup> and *N,N*-dimethylformamide (DMF),<sup>15</sup> are not stable in the radical-rich, basic, nucleophilic, and oxidizing environment of the oxygen electrode of Li-O<sub>2</sub> batteries (Figure 1). Although reformulation of classical electrolyte components, e.g., with high salt concentrations, has led to significant stability improvements in some systems, the path toward practical Li-O<sub>2</sub> batteries will most likely require the rational molecular design of novel electrolyte components.<sup>16</sup> In an early example of such an approach, Nazar and co-workers<sup>17</sup> substituted the secondary hydrogens of 1,2-dimethoxyethane (DME) with methyl groups (–CH<sub>3</sub>) to produce a new solvent with improved stability against hydrogen abstraction. More recently, ketone-based<sup>18</sup> and pivalate-based<sup>19</sup> electrolyte solvents were reported to be reasonably stable in Li-O<sub>2</sub> cells, though cycling studies were limited. Despite these examples, the rational design of electrolyte components remains an underutilized strategy for the discovery of next-generation electrolytes.

## The Bigger Picture

Lithium-oxygen (Li-O<sub>2</sub>) batteries can potentially transform energy storage and transportation with a several-fold increase in energy density over the state-of-the-art Li-ion batteries. The development of rechargeable Li-O<sub>2</sub> batteries faces substantial challenges, such as severe electrolyte instability against the highly reactive oxygen species, including superoxide, peroxide, and singlet oxygen, generated during Li-O<sub>2</sub> battery operation. To date, the vast majority of studies in this field have been based on electrolytes derived from a small set of well-studied, commercially available components (e.g., solvents such as tetraglyme and DMSO and salts such as lithium bis(trifluoromethane)sulfonimide [LiTFSI]). Although great progress has been made through optimization of such formulations, the use of physical organic chemistry principles to rationally design new molecular components may enable the discovery of electrolytes with stability profiles that cannot be achieved with existing formulations.

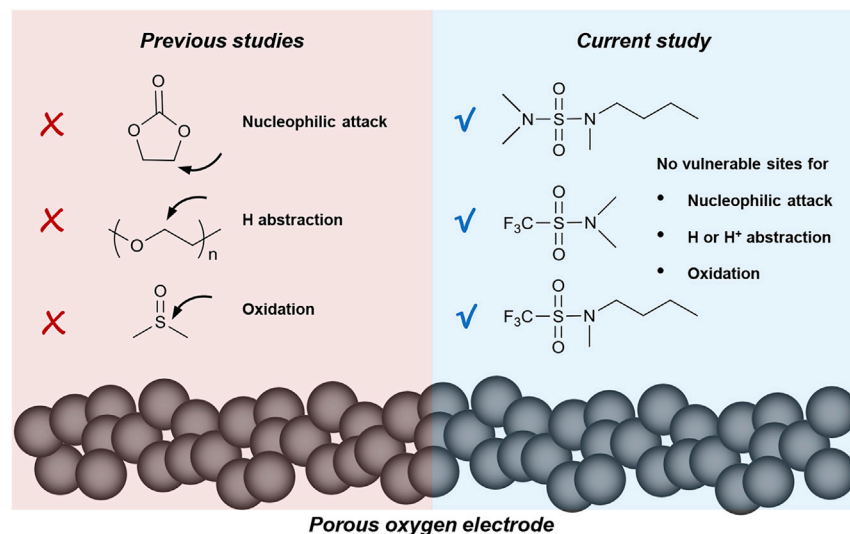


**Figure 1. Dominant Degradation Mechanisms of Carbonate-, Ether-, and Sulfoxide-Based Electrolytes and the Molecular Design of Stable Sulfamide- and Sulfonamide-Based Solvents BTMSA (Top), DMCF<sub>3</sub>SA (Middle), and BMCF<sub>3</sub>SA (Bottom) for Aprotic Li-O<sub>2</sub> Batteries**

## RESULTS AND DISCUSSION

Herein, we report three compounds—*N*-butyl-*N,N,N'*-trimethylsulfamide (BTMSA), *N,N*-dimethyl-trifluoromethanesulfonamide (DMCF<sub>3</sub>SA), and *N*-butyl-*N*-methyl-trifluoromethanesulfonamide (BMCF<sub>3</sub>SA)—that are promising for use in aprotic Li-O<sub>2</sub> batteries (Figure 1). These compounds are polar aprotic liquids at room temperature and are capable of dissolving reasonably high amounts of common Li salts, such as lithium bis(trifluoromethane)sulfonimide (LiTFSI). BTMSA has been considered as an electrolyte component for Li batteries,<sup>20</sup> and DMCF<sub>3</sub>SA was recently employed in lithium-sulfur (Li-S) batteries to suppress polysulfide solubility and shuttling.<sup>21</sup> However, the utility of these compounds as chemically and electrochemically stable electrolyte components in aprotic Li-O<sub>2</sub> batteries has not, to our knowledge, been examined. Guided by a comprehensive stability framework for organic molecules in the Li-O<sub>2</sub> oxygen electrode environment and the structure-stability relationships obtained from our previous works,<sup>16,22</sup> we designed the structures of these electrolyte components to be devoid of (1) vulnerable C–H bonds for hydrogen and proton removal, (2) electrophilic centers susceptible to nucleophilic substitution, and (3) highly electron-donating functional groups vulnerable to electrochemical oxidation. In this study, these three compounds were shown both experimentally and computationally (Figure S1) to exhibit exceptional stability toward a variety of harsh conditions encountered in the Li-O<sub>2</sub> cathode environment. For example, all three compounds were compatible with reactive species such as peroxide, superoxide, and singlet O<sub>2</sub>, whereas the trifluoromethylsulfonamides BMCF<sub>3</sub>SA and DMCF<sub>3</sub>SA displayed enhanced electrochemical oxidative stability due to the electron-withdrawing CF<sub>3</sub> group. The latter could be cycled >90 times in a Li-O<sub>2</sub> cell without capacity decay, suggesting that it could represent a significant new addition to the toolbox of electrolyte components. All together, these results highlight the power of rational molecular design for electrolyte discovery for Li-O<sub>2</sub> batteries.

We began by using a computational framework<sup>16</sup> to identify functional groups that may be stable in the Li-O<sub>2</sub> cathode environment. Sulfamides and

<sup>1</sup>Department of Chemical Engineering, Massachusetts Institute of Technology, Cambridge, MA 02139, USA

<sup>2</sup>Department of Chemistry, Massachusetts Institute of Technology, Cambridge, MA 02139, USA

<sup>3</sup>Research Laboratory of Electronics, Massachusetts Institute of Technology, Cambridge, MA 02139, USA

<sup>4</sup>Department of Mechanical Engineering, Massachusetts Institute of Technology, Cambridge, MA 02139, USA

<sup>5</sup>These authors contributed equally

<sup>6</sup>Lead Contact

\*Correspondence: [fengs@mit.edu](mailto:fengs@mit.edu) (S.F.), [jaj2109@mit.edu](mailto:jaj2109@mit.edu) (J.A.J.)

<https://doi.org/10.1016/j.chempr.2019.07.003>

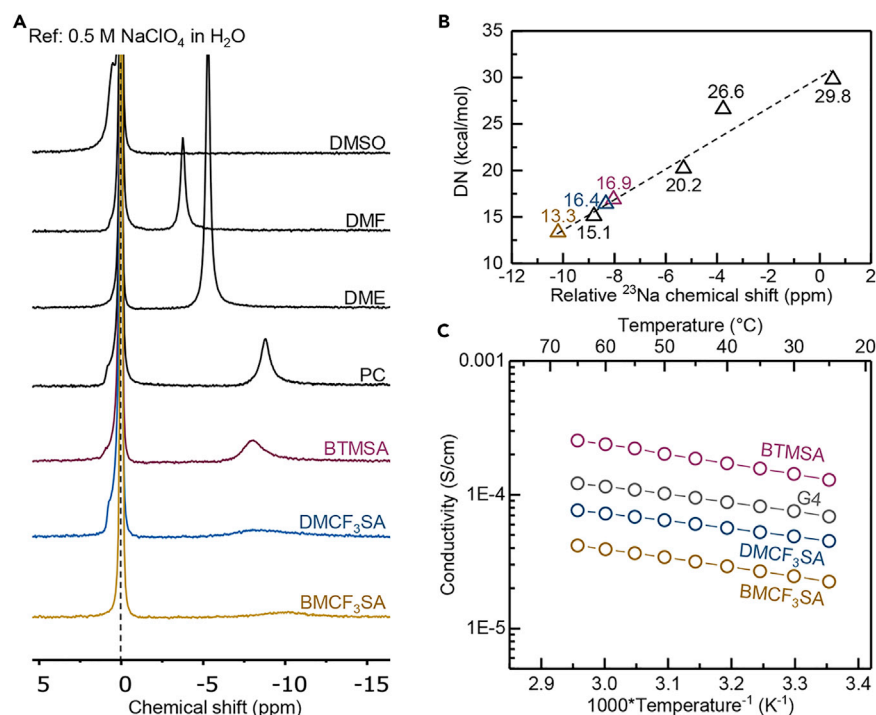


**Figure 2. Donor Number and Conductivity of BTMSA, DMCF<sub>3</sub>SA, and BMCF<sub>3</sub>SA**

(A) The measured <sup>23</sup>Na NMR chemical shifts of 20 mM NaTFSI in BTMSA, DMCF<sub>3</sub>SA, and BMCF<sub>3</sub>SA are compared with those of DMSO, DMF, DME, and PC (400 MHz). The <sup>23</sup>Na signal from the internal reference, 0.5 M NaClO<sub>4</sub> in H<sub>2</sub>O, was set to 0 ppm.

(B) A trend (dashed) line correlating the donor numbers (DNs) of DMSO (29.8 kcal/mol<sup>31</sup>), DMF (26.6 kcal/mol<sup>31</sup>), DME (20.2 kcal/mol<sup>30</sup>), and PC (15.1 kcal/mol<sup>32</sup>) and their measured relative <sup>23</sup>Na NMR shifts was used for estimating the DN of BTMSA, DMCF<sub>3</sub>SA, and BMCF<sub>3</sub>SA, which were determined to be 16.9, 16.4, and 13.3 kcal/mol, respectively.

(C) Conductivities of solutions containing 0.1 M LiTFSI in BTMSA, DMCF<sub>3</sub>SA, and BMCF<sub>3</sub>SA are compared with those of G4 as a commercial reference at various temperatures.

trifluoromethylsulfonamides lacking acidic protons and weak C–H bonds stood out as promising starting points; notably, the exceptional stability of the TFSI anionic component of the commonly used LiTFSI salt provided further motivation for exploring these scaffolds. BTMSA, BMCF<sub>3</sub>SA, and DMCF<sub>3</sub>SA were selected for further investigation: BTMSA was synthesized from *N,N*-dimethylsulfonamoyl chloride and *N*-butylmethylamine in 90% yield, whereas BMCF<sub>3</sub>SA and DMCF<sub>3</sub>SA were prepared via condensation of trifluoromethanesulfonyl chloride and the corresponding secondary amines in 80%–90% yields. These compounds are clear, colorless liquids at room temperature; their boiling temperatures, viscosities, and dielectric constants ( $\epsilon$ ) are provided in Table S1.

The donor number (DN) of an electrolyte component,<sup>23</sup> which is a quantitative descriptor of Lewis basicity, can influence the solubility<sup>24–27</sup> and lifetime<sup>24</sup> of intermediates such as LiO<sub>2</sub>,<sup>24–26</sup> as well as the discharge product morphology<sup>24,27,28</sup> and capacity of Li-O<sub>2</sub> batteries.<sup>24–27</sup> The DN of BTMSA, BMCF<sub>3</sub>SA, and DMCF<sub>3</sub>SA were estimated by <sup>23</sup>Na NMR.<sup>29</sup> Solutions of 20 mM sodium bis(trifluoromethane)sulfonimide (NaTFSI) were prepared in BTMSA, BMCF<sub>3</sub>SA, and DMCF<sub>3</sub>SA, as well as in commonly used electrolyte solvents DMSO, DMF, DME, and propylene carbonate (PC), with 0.5 M sodium perchlorate (NaClO<sub>4</sub>) in deionized water (H<sub>2</sub>O) as the internal reference. The <sup>23</sup>Na NMR shifts of NaTFSI in these seven electrolytes are shown in Figure 2A. The more upfield (more negative) <sup>23</sup>Na shifts recorded in the sulfamide- and sulfonamide-based electrolytes indicate weaker interactions between Na<sup>+</sup> and the solvation

shell in these electrolytes.<sup>29,30</sup> Using the known DNs of DMSO (29.8 kcal/mol<sup>31</sup>), DMF (26.6 kcal/mol<sup>31</sup>), DME (20.2 kcal/mol<sup>30</sup>), and PC (15.1 kcal/mol<sup>32</sup>) and their <sup>23</sup>Na NMR shifts,<sup>33</sup> we estimated the DNs of BTMSA, DMCF<sub>3</sub>SA, and BMCF<sub>3</sub>SA to be 16.9, 16.4, and 13.3 kcal/mol, respectively (Figure 2B). The low DNs of these three solvents suggest that they will have lower superoxide solubility<sup>24,26</sup> and thus higher chemical stability than high-DN solvents such as DMSO and DMF.

Because electrolytes with lower DNs coordinate with Li<sup>+</sup> more weakly, potentially leading to lower charge-carrier concentrations and conductivities (nonetheless, we note that besides the DN, solvent dielectric constant and viscosity also influence the ion conductivity), we then employed electrochemical impedance spectroscopy (EIS) to investigate the ionic conductivities of solutions containing 0.1 M LiTFSI in BTMSA, BMCF<sub>3</sub>SA, and DMCF<sub>3</sub>SA as a function of temperature, which were compared with those of tetraglyme (G4, DN = 16.6 kcal/mol<sup>30</sup>) as a reference because of its relative stability against oxygen and its reduction products (Figure 2C). The BTMSA-LiTFSI solution exhibited conductivity approximately 2-fold greater than that of G4, whereas DMCF<sub>3</sub>SA- and BMCF<sub>3</sub>SA-LiTFSI solutions had conductivities ~2- and 5-fold lower than that of BTMSA, respectively. These values can be rationalized by considering the dielectric constants ( $\epsilon$ ), DNs, and viscosities of these compounds. Although BTMSA and G4 have similar DNs and viscosities, BTMSA has a considerably higher dielectric constant than G4 (>29 versus 7.79;<sup>34</sup> Table S1) and can better screen charges, leading to overall higher charge carrier concentration and conductivity. Additionally, LiTFSI is less dissociated in DMCF<sub>3</sub>SA than BTMSA, supported by higher Raman shifts of the S-N symmetric stretching of the TFSI anion<sup>35,36</sup> (Figure S2), resulting in lower charge carrier concentration and conductivity. Furthermore, we note that BMCF<sub>3</sub>SA not only solvates Li<sup>+</sup> more weakly than DMCF<sub>3</sub>SA, leading to lower charge carrier concentration, but also has higher viscosity (Table S1), both of which contributed to its lower conductivity than DMCF<sub>3</sub>SA.

The chemical stabilities of BTMSA, DMCF<sub>3</sub>SA, and BMCF<sub>3</sub>SA were evaluated under conditions mimicking the oxygen electrode of aprotic Li-O<sub>2</sub> batteries according to a previously established protocol.<sup>16,22</sup> These electrolyte components were combined with 0.5 equiv lithium peroxide (Li<sub>2</sub>O<sub>2</sub>) and KO<sub>2</sub> powders, and the resulting mixtures were stirred at 80°C for 3 days. The lack of appreciable change in the <sup>1</sup>H NMR spectra collected before and after the exposure to Li<sub>2</sub>O<sub>2</sub> and KO<sub>2</sub> (Figures 3A–3C) indicate that these compounds are highly resistant to chemical degradation by peroxide and superoxide, in good agreement with our computational analyses (Figure S1). To account for possible solid and gas products formed during the chemical stability tests, we additionally performed quantitative NMR analyses (Figure S3; see Supplemental Information for more details) and determined that the fractions of BTMSA, BMCF<sub>3</sub>SA, and DMCF<sub>3</sub>SA remaining intact in the presence of 10 equiv Li<sub>2</sub>O<sub>2</sub> and KO<sub>2</sub> at 80°C for 3 days were 97.8%, 99.3%, and 102.1%, respectively. Overall, the quantitative NMR studies showed that these solvents were highly stable in the chemical stability tests. We note that G4 also did not yield detectable degradation products under the same test conditions. In contrast, 14.1% of the DMSO sample decomposed to form dimethyl sulfone (DMSO<sub>2</sub>), as indicated by the new resonance at ~3 ppm<sup>37</sup> (Figure 3D). Additionally, recent reports<sup>38,39</sup> have proposed electrolyte degradation due to the formation of singlet O<sub>2</sub> (<sup>1</sup>O<sub>2</sub>) during Li-O<sub>2</sub> battery operation. To investigate the reactivity of BTMSA, BMCF<sub>3</sub>SA, DMCF<sub>3</sub>SA, and DMSO with <sup>1</sup>O<sub>2</sub>, we generated <sup>1</sup>O<sub>2</sub> by irradiating solutions containing these electrolyte components as well as the photosensitizer zinc tetraphenylporphyrin (ZnTPP) in a custom-made photoreactor (Figures S4A–S4G; component list in Table S2); we verified the generation of <sup>1</sup>O<sub>2</sub> in these solutions by detecting its emission at 1,270 nm

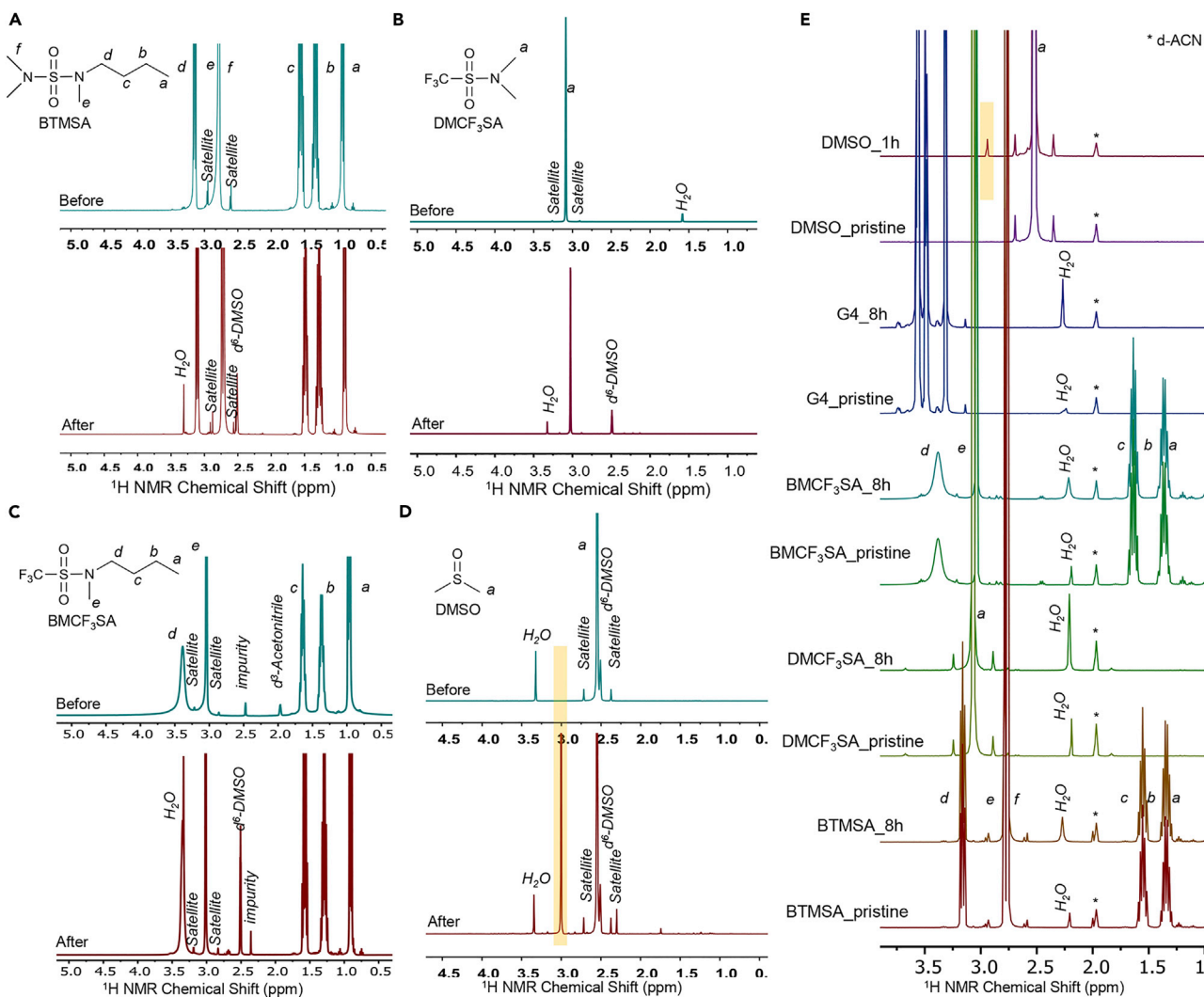


**Figure 3. Chemical Stability of BTMSA, DMCF<sub>3</sub>SA, and BMCF<sub>3</sub>SA**

(A–D) <sup>1</sup>H NMR analyses of the chemical stability of (A) BTMSA, (B) DMCF<sub>3</sub>SA, (C) BMCF<sub>3</sub>SA, and (D) DMSO. Teal and red spectra were obtained before and after the chemical stability test, respectively, in which the samples were mixed with 0.5 equiv commercial Li<sub>2</sub>O<sub>2</sub> and KO<sub>2</sub> powders. The mixtures were stirred and maintained at 80°C for 3 days.

(E) <sup>1</sup>H NMR analyses of the solutions containing 50 μL DMSO, G4, BTMSA, BMCF<sub>3</sub>SA, and DMCF<sub>3</sub>SA and 150 μM ZnTPP in 0.5 mL d-ACN before and after exposure to <sup>1</sup>O<sub>2</sub>. Length of irradiation is indicated by “\_#h” following the sample name.

(Figure S4H; see Supplemental Information for experimental details). <sup>1</sup>H NMR spectra (Figure 3E) collected before and after irradiation revealed a new resonance at ~2.94 ppm for the solution containing DMSO, whereas no observable change was observed for our synthesized compounds or G4 after 8 h of irradiation, highlighting their stability toward <sup>1</sup>O<sub>2</sub>.

We further confirmed that these electrolytes are chemically and electrochemically stable upon discharge in a real Li-O<sub>2</sub> battery environment. Li-O<sub>2</sub> cells with electrolytes containing 0.2 M LiTFSI in BTMSA, DMCF<sub>3</sub>SA, and BMCF<sub>3</sub>SA sandwiched by carbon paper with a gas diffusion layer (CP-GDL) cathode and a Li-metal anode were fully discharged at 0.03 mA/cm<sup>2</sup> with a voltage cutoff of 2.0 V<sub>Li</sub>. Cells containing electrolyte components with higher DN—BTMSA (16.9 kcal/mol) and

**DMCF<sub>3</sub>SA** (16.4 kcal/mol)—exhibited higher full discharge capacities (1.04 and 0.95 mAh/cm<sup>2</sup>, respectively, comparable to the full discharge capacities of Li-O<sub>2</sub> cells employing similar CP-GDL electrodes and a G4-based electrolyte reported previously<sup>40</sup>) than the lower-DN compound, **BMCF<sub>3</sub>SA** (DN = 13.3 kcal/mol; full discharge capacity = 0.79 mAh/cm<sup>2</sup>). This observation agrees with the previously reported trend between higher-DN electrolytes and higher discharge capacities in Li-O<sub>2</sub> batteries.<sup>24,26</sup> X-ray diffraction (XRD) characterization of CP-GDL cathodes after full discharge showed Li<sub>2</sub>O<sub>2</sub> as the discharge product (Figure S5A). After full discharge, the electrolytes were collected and analyzed by Fourier-transform infrared spectroscopy (FTIR) (Figure S5B), <sup>1</sup>H NMR (Figure S5C), and <sup>19</sup>F NMR (Figure S5D) and compared to the pristine electrolytes. No perceivable change was observed in the FTIR or NMR spectra for all three electrolytes, indicating that these electrolytes are resistant to chemical degradation under full discharge conditions. Additionally, we performed a pressure-tracking experiment to show that the ratios of electron (e<sup>-</sup>) and O<sub>2</sub> consumption during galvanostatic discharge in the G4- and **DMCF<sub>3</sub>SA**-based cells were both highly close to the 2 e<sup>-</sup>/O<sub>2</sub> ideality (Figures S6A and S6B). Furthermore, we quantified the yield of Li<sub>2</sub>O<sub>2</sub> in the G4- and **DMCF<sub>3</sub>SA**-based cells by using titration and UV-visible spectroscopy (Figures S6C and S6D; see Supplemental Information for more details). These experiments showed that the Li<sub>2</sub>O<sub>2</sub> yield in the **DMCF<sub>3</sub>SA** cell was significantly higher (85.5% ± 2.7%) than that of G4 (77.0% ± 1.7%) (Figure S6E; the yield was normalized by the total O<sub>2</sub> consumption determined in the pressure-tracking experiments; the error bars represent one standard deviation based on three replicate trials for each electrolyte), indicating that **DMCF<sub>3</sub>SA** exhibited superior discharge stability over G4.

To examine the stability of these electrolytes against charging in Li-O<sub>2</sub> batteries, we first examined the electrochemical oxidative stability of electrolytes containing 0.1 M LiTFSI in **BTMSA**, **DMCF<sub>3</sub>SA**, and **BMCF<sub>3</sub>SA** by using potentiostatic measurements, cyclic voltammetry (CV), and linear sweep voltammetry (LSV). The potentiostatic measurements were performed under an oxygenated environment in a 2-electrode electrochemical cell held at various potentials from 3.4 to 5.0 V<sub>Li</sub> for 3 h each (Figure 4A). The electrochemical cell consisted of a glass fiber separator impregnated with the electrolyte and sandwiched between a stainless-steel mesh (316) current collector and Li foil. The same measurement was performed on DMSO- and G4-based electrolytes for comparison. The sulfamide- and sulfonamide-based electrolytes exhibited high stability against electrochemical oxidation (oxidative current < 5 μA; zoomed-in view in Figure 4B) at potentials ≤ 4.5 V<sub>Li</sub>, similar to the G4-based electrolyte (Figure S6F). In contrast, the cell containing DMSO showed oxidative current that was 1~2 orders of magnitude greater. At higher potentials (≥ 4.8 V<sub>Li</sub>; Figure 4C), sulfonamides with the electron-withdrawing -CF<sub>3</sub> moiety, **BMCF<sub>3</sub>SA** and **DMCF<sub>3</sub>SA**, exhibited considerably greater electrochemical oxidative stability (oxidative current < 20 μA) than the sulfamide **BTMSA** (oxidative current 50–220 μA), in excellent agreement with our computational prediction (Figure S1). The electrochemical oxidation stability of these three electrolytes was further tested against high-surface-area carbon electrodes given that carbon-based electrodes commonly used in aprotic Li-O<sub>2</sub> batteries can participate in parasitic reactions, especially at high charging potential.<sup>41–44</sup> We performed CV (1 mV/s, 2.0–5.0 V<sub>Li</sub>; Figure S6G) tests in Ar and LSV (0.1 mV/s, from open-circuit voltage to 5.0 V; Figure S6G inset) tests in O<sub>2</sub> by using CP-GDL as the working electrode. Under both Ar and O<sub>2</sub>, the **BTMSA**- and DMSO-based electrolytes exhibited increasing oxidative current at >4.2 V<sub>Li</sub> on carbon electrodes. In contrast, the -CF<sub>3</sub> containing compounds, **BMCF<sub>3</sub>SA** and **DMCF<sub>3</sub>SA**, showed significantly improved oxidative

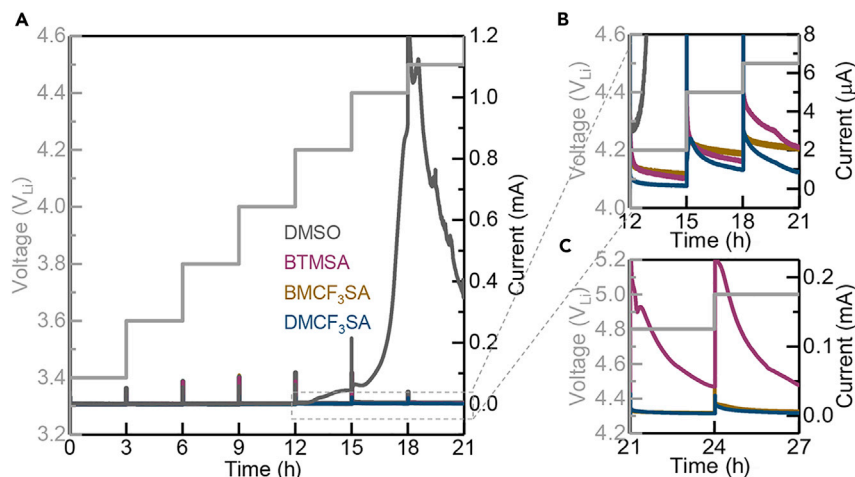


**Figure 4. Electrochemical Oxidative Stability of BTMSA, DMCF<sub>3</sub>SA, and BMCF<sub>3</sub>SA**

Potentiostatic electrochemical stability tests of electrolytes containing 0.1 M LiTFSI in BTMSA, DMCF<sub>3</sub>SA, and BMCF<sub>3</sub>SA are compared with DMSO in an oxygenated environment on stainless-steel (316) electrodes at potential  $\leq 4.5 V_{Li}$  (A); enlarged views at potential  $\geq 4.8 V_{Li}$  are shown in (B) and (C).

stability ( $>4.5 V_{Li}$ ). Notably, the oxidative current recorded in O<sub>2</sub> for the DMSO-based electrolyte was 1~2 orders of magnitude higher than that of all other electrolytes at  $5 V_{Li}$ , as shown in the Figure S6G inset.

Differential electrochemical mass spectrometry (DEMS) has been used to assess the rechargeability of Li-O<sub>2</sub> cells in various electrolytes employing carbonates, DMSO, and glymes, where deviations from the ideal  $2 e^-$  per O<sub>2</sub> stoichiometry on discharge and charge are used to quantify the (electro)chemical instability of electrolytes.<sup>10,45</sup> Generally, the rechargeability of Li-O<sub>2</sub> cells in common electrolytes follows the order of glymes  $>$  DMSO  $>$  carbonates,<sup>10,45</sup> where glyme- and carbonate-based electrolytes enable predominately O<sub>2</sub> and CO<sub>2</sub> evolution on charge,<sup>45</sup> respectively (O<sub>2</sub> evolution has also been observed in DMSO-based cells, although the rate of O<sub>2</sub> evolution is lower than that of glyme<sup>10</sup>). Here, we employed DEMS to detect gases evolved on charge under galvanostatic conditions after galvanostatic discharge of Li-O<sub>2</sub> cells by using the more electrochemically stable electrolytes, DMCF<sub>3</sub>SA and BMCF<sub>3</sub>SA (Figure 5); the recorded O<sub>2</sub> evolution rate was compared to the  $2 e^-/O_2$  ideality. Whereas the voltage profiles of the DMSO-based cell increased gradually to  $\sim 4.2 V_{Li}$  (Figure 5A), only O<sub>2</sub> was detected, and the corresponding O<sub>2</sub> evolution rate peaked at  $\sim 0.4 \mu\text{mol/h}$  and then gradually decayed, yielding an overall evolution of  $2.7 \mu\text{mol O}_2$  ( $5.2 e^-/O_2$ ). In addition to O<sub>2</sub>, significant CO<sub>2</sub> evolution was observed for the last 30% charging capacity (beginning at  $\sim 4.2 V_{Li}$  and  $\sim 0.2 \text{mAh/cm}^2$ ). In contrast, the G4- and DMCF<sub>3</sub>SA-based cells showed a long plateau at  $\sim 4.2 V_{Li}$ , which was accompanied by only O<sub>2</sub> evolution with a steady O<sub>2</sub> evolution rate of  $\sim 0.4 \mu\text{mol/h}$  (overall O<sub>2</sub> evolution =  $4.0 \mu\text{mol}$  for G4 and  $4.1 \mu\text{mol}$  for DMCF<sub>3</sub>SA, both corresponding to  $3.5 e^-/O_2$ ), as shown in Figures 5B and 5C. As the charging potential increased above  $4.3 V_{Li}$ , however, O<sub>2</sub> evolution was surpassed by CO<sub>2</sub> evolution in both G4- and DMCF<sub>3</sub>SA-based cells (Figures 5B and 5C). Whereas the charging potential of the BMCF<sub>3</sub>SA-based cell increased slowly, only O<sub>2</sub> was detected upon charging of the cell at voltages below  $4.2 V$ , where the first 70% charging capacity ( $\sim 0.2 \text{mAh/cm}^2$ ) remained below  $3.9 V_{Li}$ , after which the voltage increased steadily to  $4.3 V_{Li}$  (Figure 5D). The O<sub>2</sub> evolution rate of

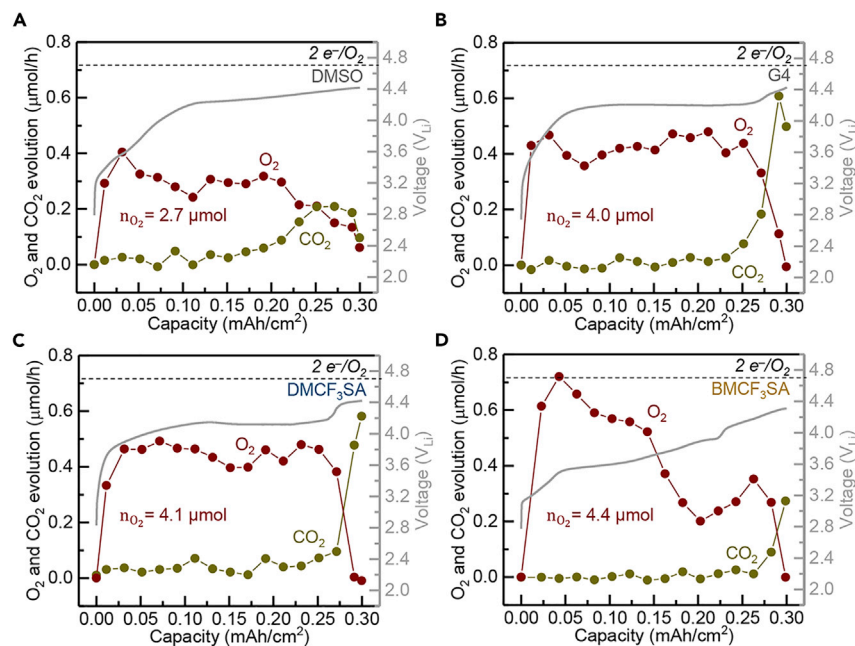


**Figure 5. Differential Electrochemical Mass Spectrometry Analysis of Li-O<sub>2</sub> Cells Employing DMSO-, G4-, DMCF<sub>3</sub>SA-, and BMCF<sub>3</sub>SA-Based Electrolytes**

Galvanostatic charging (0.03 mA/cm<sup>2</sup>) curves and gas evolution rates on charge of Li-O<sub>2</sub> cells containing 0.2 M LiTFSI in (A) DMSO, (B) G4, (C) DMCF<sub>3</sub>SA, and (D) BMCF<sub>3</sub>SA.

the BMCF<sub>3</sub>SA-based cell during the early stage of charge was approximately twice as high as the DMSO-based cell (~0.6 versus 0.3 μmol/h). As the potential of the BMCF<sub>3</sub>SA-based cell increased from 3.9 to 4.3 V<sub>Li</sub>, O<sub>2</sub> production increased again and then eventually diminished, evolving 4.4 μmol O<sub>2</sub> overall (3.2 e<sup>-</sup>/O<sub>2</sub>); CO<sub>2</sub> evolution became dominant at >4.2 V<sub>Li</sub>. We note that the overall e<sup>-</sup>/O<sub>2</sub> values for the DMSO- and G4-based cells in this work are higher than those reported previously by McCloskey et al. (5.2 versus 4.1<sup>10</sup> for DMSO and 3.5 for G4 versus 3.2<sup>45</sup> and 2.6<sup>10</sup> for DME), which is most likely due to systematic instrumentation errors. Nevertheless, these DEMS results suggest that our new electrolytes exhibit higher O<sub>2</sub> evolution efficiency and (electro)chemical stability than DMSO.

Li-O<sub>2</sub> cells employing 0.2 M LiTFSI in DMCF<sub>3</sub>SA as the electrolyte were subject to prolonged galvanostatic cycling tests (discharge at 0.03 mA/cm<sup>2</sup>, charge at 0.02 mA/cm<sup>2</sup>, and capacity cutoff at 0.1 mAh/cm<sup>2</sup> unless otherwise noted). The discharge-charge profiles of select cycles are presented in Figure 6A. The electrolytes and positive electrodes of DMCF<sub>3</sub>SA-based cells were collected after select cycles and analyzed by <sup>1</sup>H NMR (Figures 6B, S7A, and S7D; spectra of pristine electrolytes are shown in Figure S7F), <sup>19</sup>F NMR (Figures S7B and S7E), and FTIR (Figure S7C); the results were compared to those of DMSO- and G4-based cells cycled under the same galvanostatic conditions (cycling profiles in Figure S7). The <sup>1</sup>H NMR analyses (Figure 6B) revealed clear new resonances for the DMSO-based electrolyte after the first cycle (capacity cutoff = 0.3 mAh/cm<sup>2</sup>); the signal attributable to DMSO<sub>2</sub><sup>37</sup> significantly intensified after the 10<sup>th</sup> cycle (~2.9 ppm in Figures 6B and S7D). The spectrum for G4 exhibited numerous new resonances in the range of 3.6–4.7 ppm (Figure 6B) as well as a clear peak attributable to formate<sup>46,47</sup> (~8.1 ppm, Figure S7A) after 92 cycles. FTIR analyses also confirmed the presence of formate in G4-based electrolyte at ~1,700 cm<sup>-1</sup> (Figure S7C). In contrast, the

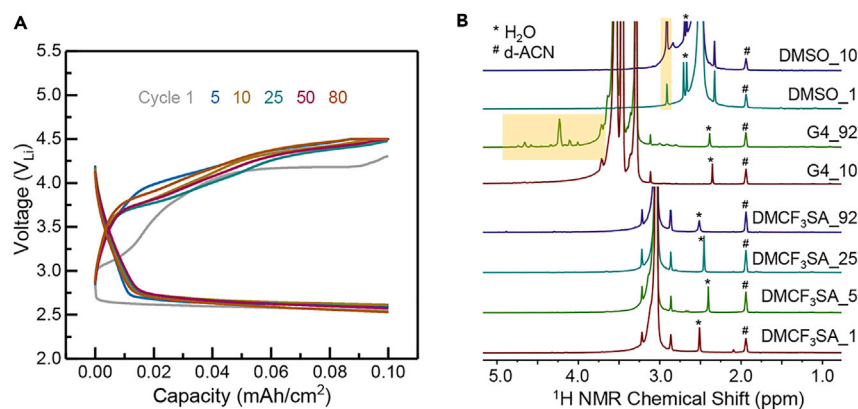


**Figure 6. Cycling Stability of Li-O<sub>2</sub> Cells Employing DMCF<sub>3</sub>SA-Based Electrolytes**

(A) Galvanostatic discharge (0.03 mA/cm<sup>2</sup>) and charge (0.02 mA/cm<sup>2</sup>) profiles of select cycles (1<sup>st</sup>, 5<sup>th</sup>, 10<sup>th</sup>, 25<sup>th</sup>, 50<sup>th</sup>, and 80<sup>th</sup> cycles) of a Li-O<sub>2</sub> cell employing 0.2 M LiTFSI in DMCF<sub>3</sub>SA as the electrolyte.

(B) <sup>1</sup>H NMR analyses on DMCF<sub>3</sub>SA-, G4-, and DMSO-based electrolytes collected after select cycles (denoted by “\_cycle#”). The asterisk (\*) indicates the signal of water from d-ACN solvent.

DMCF<sub>3</sub>SA-based electrolyte collected after the 1<sup>st</sup> (capacity cutoff = 0.3 mAh/cm<sup>2</sup>), 5<sup>th</sup>, 25<sup>th</sup>, and 92<sup>nd</sup> cycles did not display new peaks in the <sup>1</sup>H NMR (Figure 6B) and FTIR (Figure S7C) spectra, highlighting the superior stability of this electrolyte under prolonged cycling conditions. Additionally, <sup>19</sup>F NMR analysis (Figures S7B and S7E) of the DMCF<sub>3</sub>SA-based electrolyte showed a negligible change for the first 25 cycles; nonetheless, the spectrum collected after 92 cycles revealed a small amount of degradation product, most likely resulting from parasitic reactions with the Li-metal electrode and/or the oxygen electrode. Taken together, these data suggest that our electrolytes exhibit (electro)chemical stability superior to that of G4 and DMSO under prolonged cycling conditions and are promising for use in aprotic Li-O<sub>2</sub> batteries.

In summary, we present three electrolytes based on BTMSA, DMCF<sub>3</sub>SA, and BMCF<sub>3</sub>SA with enhanced chemical and electrochemical stability in aprotic Li-O<sub>2</sub> batteries. These compounds were shown to be stable in the presence of commercial Li<sub>2</sub>O<sub>2</sub> and KO<sub>2</sub> powders as well as under galvanostatic, full discharge conditions most likely because of the suppressed solubility of discharge reaction intermediates (e.g., Li<sup>+</sup>O<sub>2</sub><sup>-</sup>) resulting from low electrolyte DN<sub>s</sub>. In contrast, DMSO decomposed significantly under the same testing conditions. Additionally, BMCF<sub>3</sub>SA and DMCF<sub>3</sub>SA were considerably more stable against electrochemical oxidation (V<sub>ox</sub> > 4.5 V<sub>L</sub>) than DMSO and BTMSA, which can be attributed to the electron-withdrawing effect of the -CF<sub>3</sub> group. DEMS measurements showed O<sub>2</sub> as the vastly predominant gas evolved on charge in Li-O<sub>2</sub> cells employing sulfonamide-based electrolytes, which notably exhibited ~50% higher overall O<sub>2</sub> evolution than the DMSO cell. Li-O<sub>2</sub> cells employing the DMCF<sub>3</sub>SA-based electrolyte were cycled 90 times without capacity decay. The results presented in this study demonstrate that sulfamide- and sulfonamide-based electrolytes are promising for aprotic Li-O<sub>2</sub> battery electrolytes. In addition, this work highlights the power of molecular design in the context of Li-O<sub>2</sub> battery chemistry.

## EXPERIMENTAL PROCEDURES

### Chemical Stability Tests

A 10 mL microwave vial was charged with 0.5 mL sulfamide- or sulfonamide-based solvents with a stir bar. After three cycles of freezing, pumping, and thawing to

remove the air, the vial was transferred into the glove box. Then, 0.5 equiv Li<sub>2</sub>O<sub>2</sub> and 0.5 equiv KO<sub>2</sub> were added into the vial. After the vial was sealed, it was moved out of the glove box and heated in an oil bath at 80°C for 3 days. The reaction mixture was cooled down and treated with d<sub>6</sub>-DMSO. The mixture was further centrifuged. The liquid layer was analyzed with <sup>1</sup>H and <sup>19</sup>F NMR.

### Electrochemical Measurements

The potentiostatic oxidative stability tests (Figure 4) were conducted in an electrochemical cell consisting of either a piece of stainless-steel (316) mesh (D = 12.7 mm) or a carbon paper with gas diffusion layer electrode (CP-GDL, Freudenberg H23C2, Fuel Cells Etc, D = 12.7 mm) as the working electrode, one glass fiber separator (D = 18 MM, Whatman, Grade GF/A) impregnated with the electrolyte (0.1 M LiTFSI in the solvent of interest), and a Li foil (D = 15 mm, Chemetall, Germany). The cells were assembled in an Ar glove box (H<sub>2</sub>O < 0.1 ppm, O<sub>2</sub> < 0.1 ppm, MBraun, USA). For tests conducted in an oxygenated environment, the assembled cell was transferred to a second glove box (H<sub>2</sub>O < 1 ppm, O<sub>2</sub> < 1%, MBraun, USA) and pressurized with dry O<sub>2</sub> (99.994% purity, H<sub>2</sub>O < 2 ppm, Airgas, USA). In the potentiostatic tests, after the cell was held at open circuit voltage for 1 h, a series of potentials were applied for 3 h each: 3.4, 3.6, 3.8, 4.0, 4.2, 4.4, 4.5, 4.8, and 5.0 V<sub>Li</sub> while the current was recorded.

Galvanostatic discharge and charge (Figures 5 and 6) were performed with an electrochemical cell consisting of a CP-GDL, one glass fiber separator (D = 18 MM, Whatman, Grade GF/A) impregnated with the electrolyte (0.2 M LiTFSI in the solvent of interest), and a Li foil (D = 15 mm, Chemetall, Germany). All cells were assembled in an Ar glove box (H<sub>2</sub>O < 0.1 ppm, O<sub>2</sub> < 0.1 ppm, MBraun, USA) and pressurized with high-purity, dry O<sub>2</sub> (99.994% purity, H<sub>2</sub>O < 2 ppm, Airgas, USA) in a second glove box (H<sub>2</sub>O < 1 ppm, O<sub>2</sub> < 1%, MBraun, USA).

All electrochemical tests were conducted with a VMP3 potentiostat (BioLogic Science Instruments).

### SUPPLEMENTAL INFORMATION

Supplemental Information can be found online at <https://doi.org/10.1016/j.chempr.2019.07.003>.

### ACKNOWLEDGMENTS

The authors would like to thank the Samsung Advanced Institute of Technology for funding this research, Dr. Mounji Bawendi for his support in the photoluminescence spectroscopy experiment, and Graham Leverick for his assistance in the pressure-tracking and DEMS experiments. S.F. gratefully acknowledges the Link Foundation for an energy fellowship. J.R.L. gratefully acknowledges the National Institutes of Health for a postdoctoral fellowship (1F32GM126913-01A1). C.F.P. was supported by a National Science Foundation (NSF) graduate research fellowship under grant no. 1122374 and by the Center for Excitonics, an Energy Frontier Research Center funded by the US Department of Energy (DOE) Office of Science Basic Energy Sciences Program under award no. DE-SC0001088 (Massachusetts Institute of Technology). This research used resources of the National Energy Research Scientific Computing Center, a DOE Office of Science User Facility supported under contract no. DE-AC02-5CH11231, and the Extreme Science and Engineering Discovery Environment, which is supported by NSF grant no. ACI-1548562.

## AUTHOR CONTRIBUTIONS

Conceptualization, S.F., M.H., J.A.J., and Y.S.-H.; Methodology, S.F., M.H., W.Z., J.R.L., R.T., Y.Z., Y.G.Z., C.F.P., J.A.J., and Y.S.-H.; Investigation, S.F., M.H., W.Z., J.R.L., R.T., Y.Z., Y.G.Z., and C.F.P.; Writing – Original Draft, S.F. and M.H.; Writing – Review & Editing, S.F., M.H., W.Z., J.R.L., R.T., C.F.P., J.A.J., and Y.S.-H.; Funding Acquisition and Supervision, J.A.J. and Y.S.-H.

## DECLARATION OF INTERESTS

The authors have applied for a patent on this work.

Received: March 13, 2019

Revised: June 19, 2019

Accepted: July 3, 2019

Published: July 25, 2019

## REFERENCES AND NOTES

- Lu, J., Li, L., Park, J.B., Sun, Y.K., Wu, F., and Amine, K. (2014). Aprotic and aqueous Li-O<sub>2</sub> batteries. *Chem. Rev.* 114, 5611–5640.
- Lu, Y.-C., Gallant, B.M., Kwabi, D.G., Harding, J.R., Mitchell, R.R., Whittingham, M.S., and Shao-Horn, Y. (2013). Lithium-oxygen batteries: bridging mechanistic understanding and battery performance. *Energy Environ. Sci.* 6, 750–768.
- Christensen, J., Albertus, P., Sanchez-Carrera, R.S., Lohmann, T., Kozinsky, B., Liedtke, R., Ahmed, J., and Kojic, A. (2011). A critical review of Li/Air batteries. *J. Electrochem. Soc.* 159, R1–R30.
- Abraham, K.M., and Jiang, Z. (1996). A polymer electrolyte-based rechargeable lithium/oxygen battery. *J. Electrochem. Soc.* 143, 1–5.
- Freunberger, S.A., Chen, Y., Peng, Z., Griffin, J.M., Hardwick, L.J., Bardé, F., Novák, P., and Bruce, P.G. (2011). Reactions in the rechargeable lithium-O<sub>2</sub> battery with alkyl carbonate electrolytes. *J. Am. Chem. Soc.* 133, 8040–8047.
- Mizuno, F., Nakanishi, S., Kotani, Y., Yokoishi, S., and Iba, H. (2010). Rechargeable Li-air batteries with carbonate-based liquid electrolytes. *Electrochemistry* 78, 403–405.
- Xu, W., Xu, K., Viswanathan, V.V., Towne, S.A., Hardy, J.S., Xiao, J., Nie, Z., Hu, D., Wang, D., and Zhang, J. (2011). Reaction mechanisms for the limited reversibility of Li-O<sub>2</sub> chemistry in organic carbonate electrolytes. *J. Power Sources* 196, 9631–9639.
- Bryantsev, V.S., and Blanco, M. (2011). Computational study of the mechanisms of superoxide-induced decomposition of organic carbonate-based electrolytes. *J. Phys. Chem. Lett.* 2, 379–383.
- Freunberger, S.A., Chen, Y., Drewett, N.E., Hardwick, L.J., Bardé, F., and Bruce, P.G. (2011). The lithium-oxygen battery with ether-based electrolytes. *Angew. Chem. Int. Ed.* 50, 8609–8613.
- McCloskey, B.D., Bethune, D.S., Shelby, R.M., Mori, T., Scheffler, R., Speidel, A., Sherwood, M., and Luntz, A.C. (2012). Limitations in rechargeability of Li-O<sub>2</sub> batteries and possible origins. *J. Phys. Chem. Lett.* 3, 3043–3047.
- Wang, H., and Xie, K. (2012). Investigation of oxygen reduction chemistry in ether and carbonate based electrolytes for Li-O<sub>2</sub> batteries. *Electrochim. Acta* 64, 29–34.
- Kwabi, D.G., Batcho, T.P., Amanchukwu, C.V., Ortiz-Vitoriano, N., Hammond, P., Thompson, C.V., and Shao-Horn, Y. (2014). Chemical instability of dimethyl sulfoxide in lithium-air batteries. *J. Phys. Chem. Lett.* 5, 2850–2856.
- Mozhzhukhina, N., Méndez De Leo, L.P., and Calvo, E.J. (2013). Infrared spectroscopy studies on stability of dimethyl sulfoxide for application in a Li-air battery. *J. Phys. Chem. C* 117, 18375–18380.
- Gampp, H., and Lippard, S.J. (1983). Reinvestigation of 18-crown-6 ether/potassium superoxide solutions in Me<sub>2</sub>SO. *Inorg. Chem.* 22, 357–358.
- Chen, Y., Freunberger, S.A., Peng, Z., Bardé, F., and Bruce, P.G. (2012). Li-O<sub>2</sub> battery with a dimethylformamide electrolyte. *J. Am. Chem. Soc.* 134, 7952–7957.
- Feng, S., Chen, M., Giordano, L., Huang, M., Zhang, W., Amanchukwu, C.V., Anandakathir, R., Shao-Horn, Y., and Johnson, J.A. (2017). Mapping a stable solvent structure landscape for aprotic Li-air battery organic electrolytes. *J. Mater. Chem. A* 5, 23987–23998.
- Adams, B.D., Black, R., Williams, Z., Fernandes, R., Cuisinier, M., Berg, E.J., Novak, P., Murphy, G.K., and Nazar, L.F. (2015). Towards a stable organic electrolyte for the lithium oxygen battery. *Adv. Energy Mater.* 5.
- Sharon, D., Sharon, P., Hirshberg, D., Salama, M., Afri, M., Shimon, L.J.W., Kwak, W.J., Sun, Y.K., Frimer, A.A., and Aurbach, D. (2017). 2,4-dimethoxy-2,4-dimethylpentan-3-one: an aprotic solvent designed for stability in Li-O<sub>2</sub> cells. *J. Am. Chem. Soc.* 139, 11690–11693.
- Li, T., Wang, Z., Yuan, H., Li, L., and Yang, J. (2017). A methyl pivalate based electrolyte for non-aqueous lithium-oxygen batteries. *Chem. Commun.* 53, 10426–10428.
- Choquette, Y. (1998). Sulfamides and glymes as aprotic solvents for lithium batteries. *J. Electrochem. Soc.* 145, 3500.
- Shyamsunder, A., Beichel, W., Klose, P., Pang, Q., Scherer, H., Hoffmann, A., Murphy, G.K., Krossing, I., and Nazar, L.F. (2017). Inhibiting polysulfide shuttle in lithium-sulfur batteries through low-ion-pairing salts and a Triflamide solvent. *Angew. Chem. Int. Ed.* 56, 6192–6197.
- Huang, M., Feng, S., Zhang, W., Giordano, L., Chen, M., Amanchukwu, C.V., Anandakathir, R., Shao-Horn, Y., and Johnson, J.A. (2018). Fluorinated aryl sulfonimide tagged (FAST) salts: modular synthesis and structure-property relationships for battery applications. *Energy Environ. Sci.* 11, 1326–1334.
- Gutmann, V. (1976). Solvent effects on the reactivities of organometallic compounds. *Coord. Chem. Rev.* 18, 225–255.
- Abraham, K.M. (2015). Electrolyte-directed reactions of the oxygen electrode in lithium-air batteries. *J. Electrochem. Soc.* 162, A3021–A3031.
- Aetukuri, N.B., McCloskey, B.D., Garcia, J.M., Krupp, L.E., Viswanathan, V., and Luntz, A.C. (2015). Solvating additives drive solution-mediated electrochemistry and enhance toroid growth in non-aqueous Li-O<sub>2</sub> batteries. *Nat. Chem.* 7, 50–56.
- Johnson, L., Li, C., Liu, Z., Chen, Y., Freunberger, S.A., Ashok, P.C., Praveen, B.B., Dholakia, K., Tarascon, J.M., and Bruce, P.G. (2014). The role of LiO<sub>2</sub> solubility in O<sub>2</sub> reduction in aprotic solvents and its consequences for Li-O<sub>2</sub> batteries. *Nat. Chem.* 6, 1091–1099.
- Kwabi, D.G., Batcho, T.P., Feng, S., Giordano, L., Thompson, C.V., and Shao-Horn, Y. (2016). The effect of water on discharge product growth and chemistry in Li-O<sub>2</sub> batteries. *Phys. Chem. Chem. Phys.* 18, 24944–24953.
- Aurbach, D., Daroux, M., Faguy, P., and Yeager, E. (1991). The electrochemistry of noble metal electrodes in aprotic organic solvents containing lithium salts. *J. Electroanal. Chem.* 297, 225–244.

29. Erlich, R.H., and Popov, A.I. (1971). Spectroscopic studies of ionic solvation. X. Study of the solvation of sodium ions in nonaqueous solvents by sodium-23 nuclear magnetic resonance. *J. Am. Chem. Soc.* **93**, 5620–5623.
30. Burke, C.M., Pande, V., Khetan, A., Viswanathan, V., and McCloskey, B.D. (2015). Enhancing electrochemical intermediate solvation through electrolyte anion selection to increase nonaqueous Li-O<sub>2</sub> battery capacity. *Proc. Natl. Acad. Sci. USA* **112**, 9293–9298.
31. Linert, W., Jameson, R.F., and Taha, A. (1993). Donor numbers of anions in solution: the use of solvatochromic Lewis acid-base indicators. *J. Chem. Soc. Dalton Trans.* **3181**, 3181–3186.
32. Cahen, Y.M., Handy, P.R., Roach, E.T., and Popov, A.I. (1975). Spectroscopic studies of ionic solvation. XVI. Lithium-7 and chlorine-35 nuclear magnetic resonance studies in various solvents. *J. Phys. Chem.* **79**, 80–85.
33. Handy, P.R., and Popov, A.I. (1972). Spectroscopic studies of ionic solvation—XII. *Spectrochim. Acta A* **28**, 1545–1553.
34. Rivas, M.A., Iglesias, T.P., Pereira, S.M., and Banerji, N. (2006). On the permittivity and density of the systems {tetraglyme + (n-nonane or n-dodecane)} at various temperatures. *J. Chem. Thermodyn.* **38**, 245–256.
35. Tataru, R., Kwabi, D.G., Batcho, T.P., Tulodziecki, M., Watanabe, K., Kwon, H.-M., Thomas, M.L., Ueno, K., Thompson, C.V., Dokko, K., et al. (2017). Oxygen reduction reaction in highly concentrated electrolyte solutions of lithium bis(trifluoromethanesulfonyl)amide/dimethyl sulfoxide. *J. Phys. Chem. C* **121**, 9162–9172.
36. Umebayashi, Y., Mitsugi, T., Fukuda, S., Fujimori, T., Fujii, K., Kanzaki, R., Takeuchi, M., and Ishiguro, S.-I. (2007). Lithium ion solvation in room-temperature ionic liquids involving bis(trifluoromethanesulfonyl) imide anion studied by Raman spectroscopy and DFT calculations. *J. Phys. Chem. B* **111**, 13028–13032.
37. Weber, M., Hellriegel, C., Rueck, A., Wuethrich, J., and Jenks, P. (2014). Using high-performance <sup>1</sup>H NMR (HP-qNMR®) for the certification of organic reference materials under accreditation guidelines—describing the overall process with focus on homogeneity and stability assessment. *J. Pharm. Biomed. Anal.* **93**, 102–110.
38. Mahne, N., Schafzahl, B., Leypold, C., Leypold, M., Grumm, S., Leitgeb, A., Strohmeier, G.A., Wilkening, M., Fontaine, O., Kramer, D., et al. (2017). Singlet oxygen generation as a major cause for parasitic reactions during cycling of aprotic lithium-oxygen batteries. *Nat. Energy* **2**, 1–9.
39. Wandt, J., Jakes, P., Granwehr, J., Gasteiger, H.A., and Eichel, R.A. (2016). Singlet oxygen formation during the charging process of an aprotic lithium-oxygen battery. *Angew. Chem. Int. Ed.* **55**, 6892–6895.
40. Gao, X., Chen, Y., Johnson, L., and Bruce, P.G. (2016). Promoting solution phase discharge in Li-O<sub>2</sub> batteries containing weakly solvating electrolyte solutions. *Nat. Mater.* **15**, 882–888.
41. Gallant, B.M., Mitchell, R.R., Kwabi, D.G., Zhou, J., Zuin, L., Thompson, C.V., and Shao-Horn, Y. (2012). Chemical and morphological changes of Li-O<sub>2</sub> battery electrodes upon cycling. *J. Phys. Chem. C* **116**, 20800–20805.
42. Itkis, D.M., Semenenko, D.A., Kataev, E.Y., Belova, A.I., Neudachina, V.S., Sirotnina, A.P., Hävecker, M., Teschner, D., Knop-Gericke, A., Dudin, P., et al. (2013). Reactivity of carbon in lithium-oxygen battery positive electrodes. *Nano Lett.* **13**, 4697–4701.
43. McCloskey, B.D., Speidel, A., Scheffler, R., Miller, D.C., Viswanathan, V., Hummelshøj, J.S., Nørskov, J.K., and Luntz, A.C. (2012). Twin problems of interfacial carbonate formation in nonaqueous Li-O<sub>2</sub> batteries. *J. Phys. Chem. Lett.* **3**, 997–1001.
44. Ottakam Thotiyil, M.M., Freunberger, S.A., Peng, Z., and Bruce, P.G. (2013). The carbon electrode in nonaqueous Li-O<sub>2</sub> cells. *J. Am. Chem. Soc.* **135**, 494–500.
45. McCloskey, B.D., Bethune, D.S., Shelby, R.M., Girishkumar, G., and Luntz, A.C. (2011). Solvents' critical role in nonaqueous lithium-oxygen battery electrochemistry. *J. Phys. Chem. Lett.* **2**, 1161–1166.
46. Nasybulin, E., Xu, W., Engelhard, M.H., Nie, Z., Burton, S.D., Cosimbescu, L., Gross, M.E., and Zhang, J.-G. (2013). Effects of electrolyte salts on the performance of Li-O<sub>2</sub> batteries. *J. Phys. Chem. C* **117**, 2635–2645.
47. McCloskey, B.D., Valery, A., Luntz, A.C., Gowda, S.R., Wallraff, G.M., Garcia, J.M., Mori, T., and Krupp, L.E. (2013). Combining accurate O<sub>2</sub> and Li<sub>2</sub>O<sub>2</sub> assays to separate discharge and charge stability limitations in nonaqueous Li-O<sub>2</sub> batteries. *J. Phys. Chem. Lett.* **4**, 2989–2993.